

Supporting Information

Highly conductive and porous activated reduced graphene oxide films for high-power supercapacitors

Li Li Zhang,⁺ Xin Zhao,^{+‡} Meryl D. Stoller,⁺ Yanwu Zhu,^{+§} Hengxing Ji,⁺ Shanthi Murali,⁺ Yaping Wu,⁺ Stephen Perales,⁺ Brandon Cleveger,⁺ Rodney S. Ruoff^{*+}

⁺Department of Mechanical Engineering and the Materials Science and Engineering

Program, The University of Texas at Austin, One University Station C2200, Austin, TX
78712

[‡]State Key Laboratory for Modification of Chemical Fibers and Polymer Materials,

College of Materials Science and Engineering, Donghua University, Shanghai, 201620, P.
R. China

[§]Department of Materials Science and Engineering, University of Science and

Technology of China, Hefei, 230036, P. R. China.

Email: r.ruoff@mail.utexas.edu

Experimental details

1. Synthesis of aG-O film

The graphene oxide (G-O) colloidal dispersion was prepared by sonication of graphite oxide (GO), which was obtained from natural graphite using a modified Hummers

method. The colloidal solution which contained G-O platelets suspended in water with KOH dissolved in the water was obtained by addition of 1M KOH dropwise into 1 mg/ml of G-O colloidal suspension. The mass ratio of KOH to G-O was varied to be 10, 12, 14, and 16 to control the degree of activation. The water in the colloidal solution was then evaporated in an oil bath at 100 °C under constant stirring until it thickened into an ‘ink-paste’. The precursor G-O/KOH films were deposited onto a PTFE membrane (SterliTech) as a paste that was rapidly dried by brief vacuum filtration under directional flow followed by drying at 80 °C in ambient for 24 hours.

The activation process has been previously reported.¹ Briefly, the dry precursor G-O/KOH film was first heated at 280 °C for 30 minutes, the temperature was ramped at 5 °C/min to 800 °C and held there for 1 hour in a horizontal tube furnace (50-mm diameter), with an argon flow of 150 sccm at a pressure of one atmosphere. The sample was allowed to cool down over a period of several hours, removed from the furnace and repeatedly washed with 10 wt% acetic acid and de-ionized water until a pH value of 7 was reached. The final aG-O film was obtained after drying at 80 °C in ambient for 24 hours.

2. General characterization

The microscopic feature of the samples was observed with scanning electron microscopy (SEM, Hitachi S5500, 30kV) and transmission electron microscopy (TEM, JEOL 2010F, 200 kV). The pore structure of the sample was investigated using physical adsorption of nitrogen at the liquid-nitrogen temperature (77 K) on an automatic volumetric sorption analyzer (NOVA2000, Quantachrome). Prior to measurement, a sample was vacuum-degassed at room temperature for 5 h. The specific surface area (S_{BET}) was determined

according to the Brunauer–Emmett–Teller (BET) method in the relative pressure range of 0.05 – 0.2. X-ray photoelectron spectroscopy (XPS) was conducted on an AXIS Ultra DLD system (Kratos Analytical) equipped with a monochromatic Al K α X-ray source (1486.6 eV). Combustion elemental analysis was done at Atlantic Microlab, Inc. (Georgia, USA) for determination of the C, O, and H content. The electrical conductivity of aG-O films was obtained by the method described in Ref (1).

3. Supercapacitor measurements

A two-electrode cell configuration was used to measure the performance of aG-O films as supercapacitor electrodes. The aG-O films were directly punched into 0.5 inch diameter electrodes with thicknesses ranging from 7 to 30 μm . No binder or conductive additives were used. Two nearly identical (by weight and size) film electrodes were assembled in a test cell consisting of two current collectors, two electrodes, and an ion-porous separator (Celgard® 3501) supported in a test fixture consisting of two stainless steel plates.

Gravimetric capacitance for a single electrode was calculated from galvanostatic charge/discharge as

$$C_{single} = \frac{I\Delta t}{m\Delta V}$$

where I is the constant current and m is the total mass for both carbon electrodes, Δt is the discharge time and ΔV is the voltage change during the discharge process.

The energy density was estimated by using the formula

$$E = \frac{C_{single} V^2}{8}$$

Effective series resistance (ESR) was estimated using the voltage drop at the beginning of the discharge, V_{drop} , at certain constant current I , with the formula

$$R_{ESR} = \frac{V_{drop}}{2I}$$

The power density, calculated from the discharge data at certain constant current I and normalized with the weight of the cell (two electrodes) is given by

$$P = \frac{(V_{max} - V_{drop})^2}{4R_{ESR}m}$$

Figures/Tables

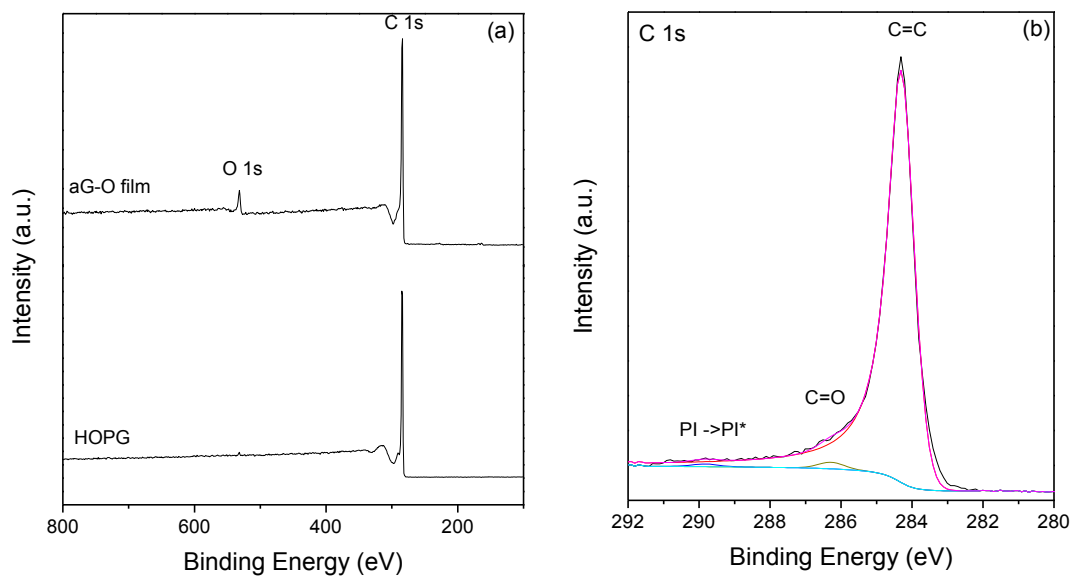


Figure S1. (a) XPS spectrum of aG-O14 in comparison to that of HOPG and (b) the C1s spectrum of aG-O14.

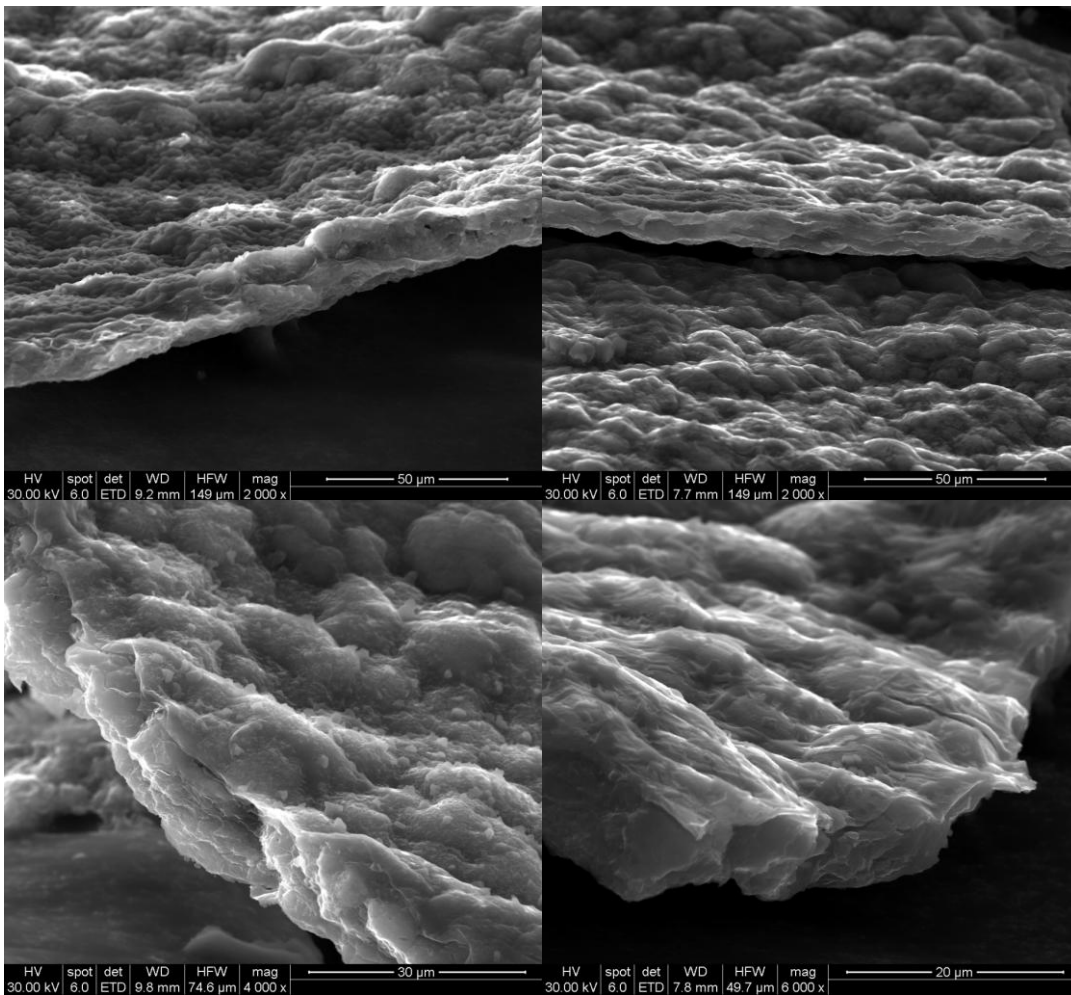


Figure S2. SEM images of precursor G-O/KOH films.



Figure S3. Precursor G-O/KOH 'cakes' and delaminated G-O/KOH papers obtained from non-homogenous G-O/KOH solutions.

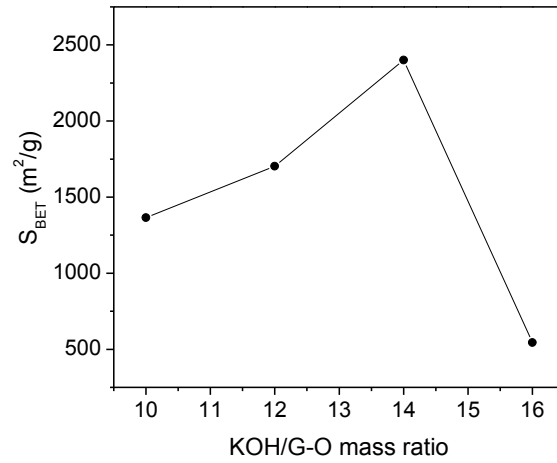
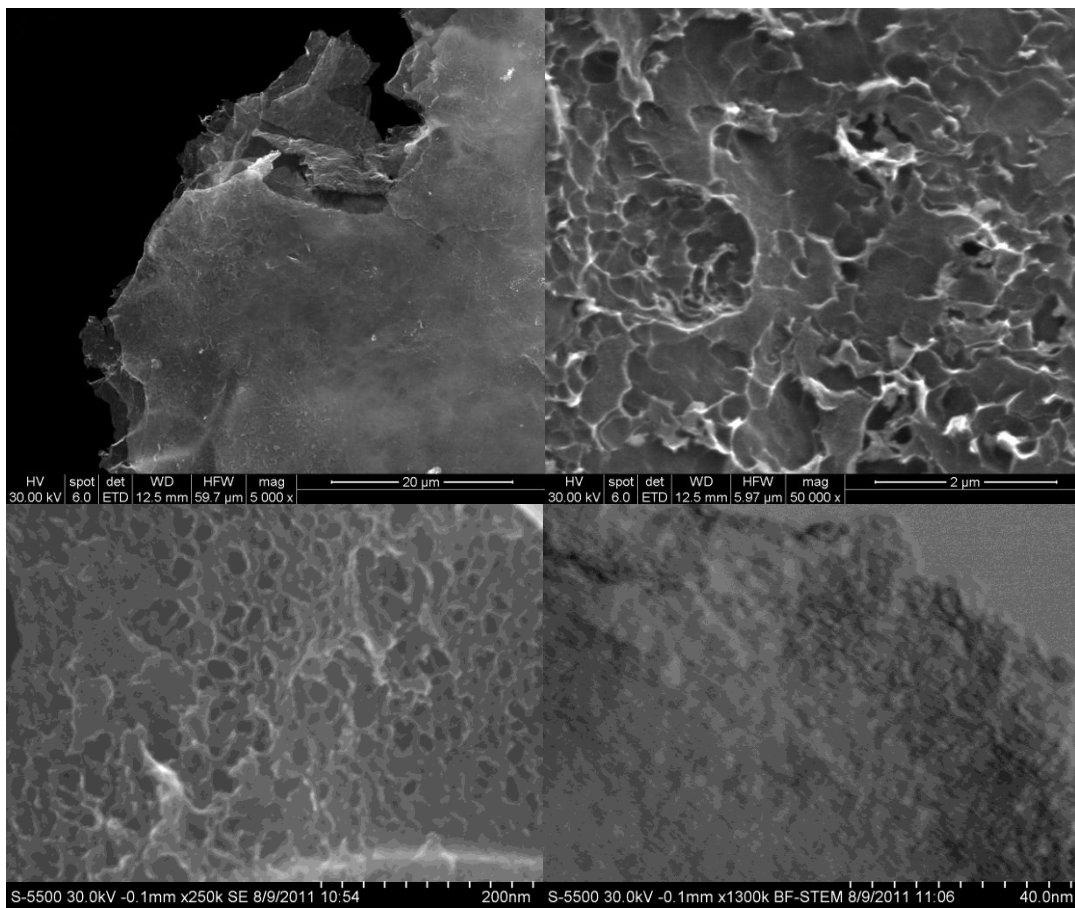


Figure S4. The BET specific surface area of aG-O films as a function of KOH to G-O mass ratio. (Lines connecting points are only a guide to the eye.)



FigureS5. High-resolution SEM and BF-STEM images of aG-O16 film demonstrating the etching/digesting of the carbon film with excessive KOH activation.

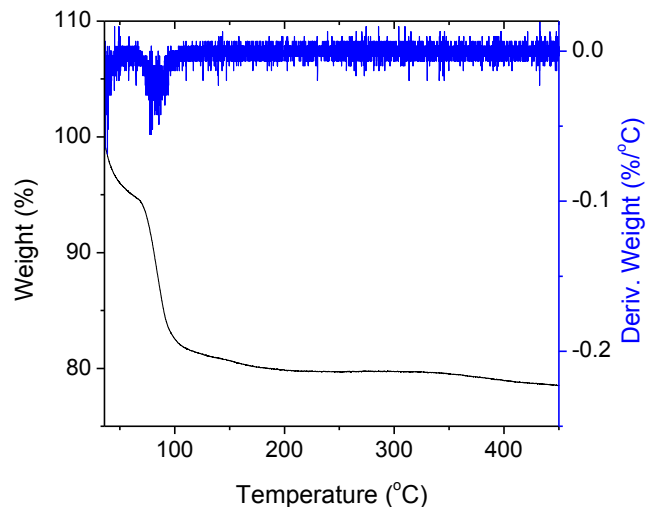


Figure S6. Weight loss curve and derivative weight loss curve for the precursor G-O/KOH film. The weight loss between 70 and 100°C is due to the water adsorbed by the precursor film from the air. There is little weight loss (< 5wt%) between 100 and 300°C (which is where there is a well known weight loss of O-containing functional groups from graphite oxide), indicating the removal of most of the O-containing functional groups by KOH during the evaporation process.

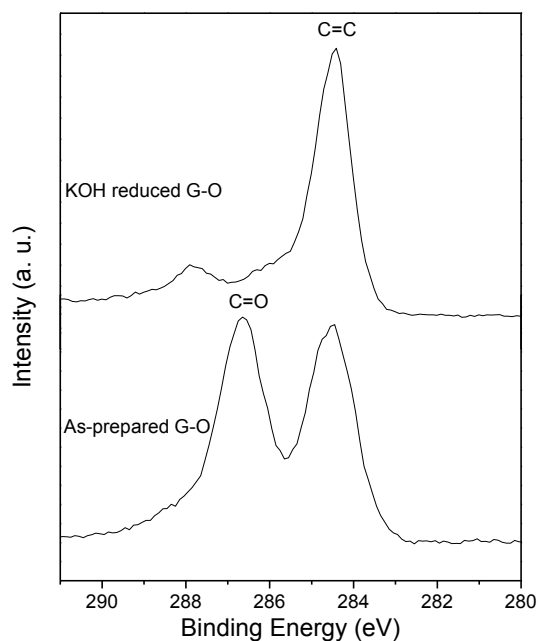


Figure S7. XPS spectra of the C 1s region of (upper) KOH reduced G-O and (lower) as-prepared G-O.

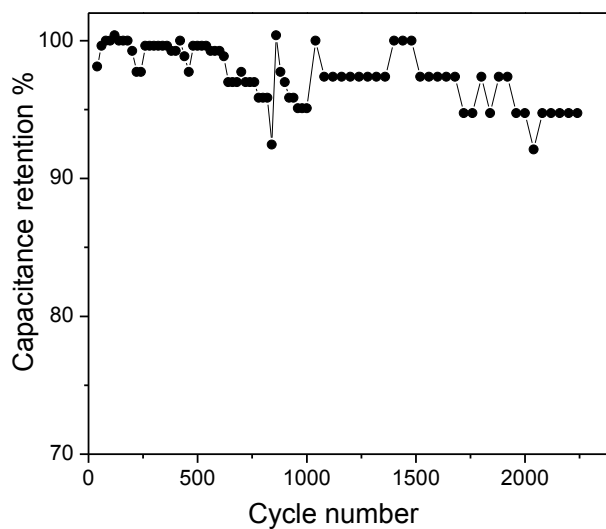


Figure S8. Cycling performance of aG-O14 film at a current density of 20A/g in 1 M KOH solution.

1. Zhu, Y.; Murali, S.; Stoller, M. D.; Ganesh, K. J.; Cai, W.; Ferreira, P. J.; Pirkle, A.; Wallace, R. M.; Cychosz, K. A.; Thommes, M.; Su, D.; Stach, E. A.; Ruoff, R. S. *Science* **2011**, 332, (6037), 1537-1541.